PCCP

Accepted Manuscript




ROYAL SOCIETY OF CHEMISTRY

www.rsc.org/pccp

Cite this: DOI: 10.1039/c0xx00000x

www.rsc.org/xxxxxx

ARTICLE TYPE

# Dynamics of supercooled water in a biological model system of the amino acid L-lysine

**Silvina Cerveny,*[a] and Jan Swenson[a,b]**

***Received (in XXX, XXX) Xth XXXXXXXXX 20XX, Accepted Xth XXXXXXXXX 20XX***

**DOI: 10.1039/b000000x**

The dynamics of supercooled water in aqueous solutions of the single amino acid L-lysine has been studied by broadband dielectric spectroscopy. The chosen biological system is unique in the sense that the water content is high enough to fully dissolve the amino acid, but low enough to avoid crystallisation to ice at any temperature. This is not possible to achieve for proteins or other larger biomolecules, where either hydrated samples without ice or solutions with large quantities of ice, or a cryoprotectant sugar, have to be studied at low temperatures. Thus, it is a key finding to be able to study water and biomolecular dynamics in a non-crystallized and biologically realistic solution at supercooled temperatures. Here, we focus on the water dynamics in this unique biological solution of L-lysine and water. We show that this unique system also gives rise to unique water dynamics, since, for the first time, a continuation of a cooperative ($\alpha$-like) water relaxation is observed after a crossover to a more local $\beta$-like water relaxation has occurred with decreasing temperature. This implies that the supercooled water in the biological solution shows a twofold relaxation behaviour, with one relaxation identical to the main relaxation of water in hard confinements and one relaxation almost identical to the main water relaxation in ordinary aqueous solutions.

## INTRODUCTION

Water in solutions and under nano-confinement has enormous importance not only in biological systems but also in fundamental and applied research. Therefore, a large number of experimental and simulation investigations have been performed to characterize water properties in different environments, such as close to hydrophilic or hydrophobic surfaces, trapped in nano-cavities, in mixtures with liquids and polymers, etc. In addition, it is widely recognized that water significantly influences the dynamics, functionality, structure and stability of proteins and therefore it manage the life itself[1-6]. However, the effects imposed by a biomolecule on water dynamics are exceptionally complex, due to the variety of polar and non-polar side chains present in the biosystem. In fact, the range of possible solvating interfaces can be enormous, which makes it difficult to experimentally determine the water dynamics in each environment. To at least partly overcome this difficulty it is common to study water dynamics in less complex model systems, such as porous silica matrixes[7-11], solutions of relatively simple molecules (e.g. amphiphilic peptides[12-15] or single amino acids[16]) or even solutions of non-biological systems (ordinary solutions such as polymers[17, 18], carbohydrates[19, 20], etc). By using this approach, both general insights about hydration water and more specific information about how water behaves in different types of environments have been gained, although the use of simplified model systems has also received some criticisms[21].

Studies of the dynamical properties of water in solutions of larger biomolecules, such as proteins, at supercooled temperatures have, however, some experimental difficulties. The aqueous solvent will unavoidably crystallize below 235 K, preventing the possibility to study the dynamics of amorphous water at low temperatures. In addition, the study of proteins and associated water in a biologically realistic environment has the problem of the low solubility of proteins in pure water. This fact makes the dynamical behaviour of the solvent almost totally dominated by its bulk properties, while the dynamics of water molecules at the interface give a too weak contribution to be reliably determined in such studies. Due to these limitations of studying proteins solvated in water it has become more common to study just hydrated powders of the proteins, where ice formation can be avoided at all temperatures for $h$-values up to about 0.4 ($h$ is g of water per g of protein)[22]. However, studies of hydrated powders have also their obvious limitations since they are not representative of a genuine biological environment. Even in solutions of small peptides, sometimes used as model systems, water crystallize on cooling[12], preventing the study of water dynamics at low temperatures. Thus, several factors actually limit

a detailed experimental investigation of the relation between water and protein dynamics.

Due to these limitations of studying protein-water systems (or similar systems of larger biomolecules) we have taken another approach and studied the dynamics of a biological system containing the relatively small amino acid L-lysine. L-lysine is a necessary building block of all proteins of animals and it plays a major role in calcium absorption, the building of muscle protein, and the recovering from surgery. Lys residues play key roles in Alzheimer's disease, because they participate in a combination of hydrophobic and electrostatic interactions that leads to the formation of toxic oligomers and aggregates by multiple disease-related proteins[23]. Moreover, a low L-lysine diet decreases the concentrations of glutaric acid in brain, liver, kidney and serum, and this may lead to brain damage during infancy[24]. Thus, in spite of the fact that lysine is a single amino acid, it is involved in various biological functions. In a water solution at pH ≈ 10, the carboxyl group of lysine is deprotonated ($COO^-$) and both amino groups ($NH_3^+$) are protonated. This latter group contributes to protein stability and it is crucial for ubiquitin function[25]. Furthermore, L-lysine has no methyl group ($CH_3$), which often gives a substantial contribution to the dynamics of hydrated proteins when studied by neutron scattering, and may mask the response of the water dynamics[26]. However, the greatest advantage of the L-lysine-water system is the possibility to cover a large water concentration range ($c_w$ varying between 5 and 40 wt%) from a hydrated powder to a clear and transparent solution, without any crystallization on cooling/heating. This contrasts the possibility of protein studies, where only hydrated powders can be explored at low temperatures without crystallization.

In this work we have been able to perform a dielectric relaxation study of L-lysine when it is fully dissolved in water, without having any problem of crystallization at any temperature. This contrasts normal studies of proteins or peptides in which hydrated powders are analysed. Finally, we have made a critical comparison of the water dynamics in different environments (such as ordinary solutions and water in hard confinements) and discussed the unique relaxation behaviour observed in this study.

## EXPERIMENTAL

L-lysine ($M_n$ = 146.19 g/mol) and ultrapure water from Aldrich Chemical Co. Inc., were used without any further purification. Water contents will be expressed in two ways: $h$ (grams of water per gram of lysine) or $c_w$ (weight percentage). For the preparation of the hydrated powder, dried lysine was hydrated in $H_2O$ atmosphere at two different levels, $h$ = 0.05 ($c_w$ = 5 wt%) and $h$ = 0.10 ($c_w$ = 9 wt%). Both levels represent less than one water molecule per amino acid, 0.4 and 0.8 respectively. For the preparation of the rest of the samples, water was added to reach the levels of $h$ given in Table I. The mixtures were then sealed during one week in order to achieve a good water distribution. Whereas samples with $0.43 < h < 0.66$ are clear and transparent solutions, samples with $0.10 < h < 0.25$ $h$ are opaque and they turned to a gel-like consistency. This broad range of concentrations allows analysing the binary system lysine-water, from a hydrated powder to a transparent solution (see Table I). Note that the concentration range explored in this work contrasts the study of our previous work[16], in which well-diluted solutions were analysed.

Differential scanning calorimetry measurements were performed by means of a DSC Q-2000 from TA Instruments, using cooling and heating rates of 10 K/min. From the heat flow/temperature curves, the glass transition temperature ($T_g$) was calculated as the onset point. On cooling no sign of crystallization was found for any sample (figure S1 in Supplementary information shows the calorimetric response for the highest water contents analysed in this work). On heating, all samples revealed a single $T_g$, which was very narrow (≈ 5 degrees) in contrast to hydrated proteins[22, 27, 28].

To measure the complex dielectric permittivity, $\varepsilon''(\omega) = \varepsilon(\omega) - i\,\varepsilon''(\omega)$, we combined different dielectric techniques to obtain a wide spectral range (0.1 Hz to 20 GHz). For the frequency range from $10^{-1}$ Hz to $10^6$ Hz, we used a Novocontrol Alpha- Analyser, whereas for the frequency range from $10^6$ Hz to $10^9$ Hz, an Agilent rf impedance analyser 4192B was used. The sample thickness was for all measurements 0.1 mm, and the sample diameter was 30 mm and 10 mm for the low and high frequency measurements, respectively. Each sample was placed in a sample holder and cooled down to 150 K and then reheated to 300 K while isothermal (±0.1 K) scans were made at every third degree and 2.5 degree over the temperature ranges 150 − 190 K and 192.5 − 300K, respectively. To ensure that no crystallization occurs during the time of the dielectric experiment (a very low heating rate is used) we measured the same sample also on cooling. We observed that the dielectric signal remains the same in both cycles and this implies that there is no crystallization (even partial crystallization) during the dielectric measurements. Finally, in the frequency range of 0.2–20 GHz a dielectric probe kit Hewlett-Packard (HP) HP-85070E (bandwidth 200 MHz to 20 GHz) with an open ended coaxial probe connected to a vector analyser (VNA) HP-8361 was used to measure the dielectric permittivity at room temperature (295.15K).

To analyse the complex permittivity ($\varepsilon^*$), simultaneous fitting of both real ($\varepsilon'$) and imaginary ($\varepsilon'$) components were performed. The dielectric response of the mixtures can be well described by using standard fit functions. We used the well-known Cole-Cole function[29] to describe each relaxation process,

$$\varepsilon^*(\omega) = \varepsilon_\infty + \frac{\Delta\varepsilon}{1+(i\omega\tau)^\alpha} \quad (1)$$

where $\Delta\varepsilon$ is the dielectric strength ($\Delta\varepsilon = \varepsilon_s - \varepsilon_\infty$, $\varepsilon_\infty$ and $\varepsilon_s$ are the unrelaxed and relaxed values of the dielectric constant), $\tau$ is the relaxation time and $\alpha$ is the stretching parameter of each relaxation process and $\omega = 2\pi f$ is the angular frequency. Over the whole temperature range explored we found five relaxation processes (although only up to three relaxations coexist in the frequency window at each temperature). The total fit function was given by:

$$\varepsilon^*(\omega) = \varepsilon_\infty + \sum_j \frac{\Delta\varepsilon_j}{1+(i\omega\tau_j)^{\alpha_j}} - i\left(\frac{\sigma}{\varepsilon_o\omega}\right)^N \quad (2)$$

In addition, at low frequencies conductivity effects dominate, and to account for that a power law term was added (last term in eq. (2)), where $\varepsilon_0$ denotes the vacuum permittivity and $\sigma$ is the static ionic conductivity.

Thermo Stimulated Depolarization Current (TSDC) is a dielectric technique in the temperature domain. An electric field is applied at a certain temperature ($T_p$) for a short time (1 min). With the electric field still applied, the sample is cooled to a temperature $T_o$, which is sufficiently low to prevent depolarization by thermal energy and to ensure that the relaxation times are longer than the measuring time. Then the sample is short-circuited and reheated at a constant rate $q$ while the discharge current is measured as a function of temperature. TSDC measurements were carried out using a Keithley 6517 in combination with a Novocontrol sample cell for TSDC measurements. Experimental conditions were $T_p$ = 183 K, $T_o$ = 140 K, and heating rates ($q$) of 0.5, 1, 3, 5, 7, 10 K/min.

***Table I.*** General characterization of the samples. $c_w$ is the weight fraction of water, h expresses the water content in grams of water per gram of dry lysine, $T_g$, DSC represents the calorimetric glass transition temperature, $\rho$ is the density, $N$ is the number of water molecules per lysine molecule

| Sample | Sample type | $c_w$ | h | $T_{g,DSC}$ [K] | ρ [g/cm$^3$] | pH | N |
|---|---|---|---|---|---|---|---|
| L60-W40 | solution | 40 | 0.66 | 194.2 | 1.14 | 10.5 | 5.4 |
| L65-W35 | solution | 35 | 0.53 | 198.2 | 1.15 | 10.8 | 4.4 |
| L70-W30 | solution | 30 | 0.43 | 205.6 | 1.16 | 10.9 | 3.6 |
| L80-W20 | Gel-like | 20 | 0.25 | 206.7 | 1.18 | 11.0 | 2.0 |
| L91-W09 | Gel-like | 9 | 0.10 | 212.3 | --- | --- | 0.8 |
| L95-W05 | Hydrated powder | 5 | 0.05 | --- | --- | --- | 0.4 |

## RESULTS ON LYSINE-WATER MIXTURES

Figure 1 shows both components of the complex dielectric permittivity data for the mixture with $c_w$ = 40 wt% at a temperature below $T_g$. (figure 1(a) and (b)) and at a temperature above $T_g$ (figure 1(c) and (d)). In addition, figure S2 in Supplementary Information shows the dielectric response at several temperatures for the same sample, where the gradual change from low to high temperature data can be observed. Note that broadband dielectric spectroscopy (BDS) is a technique based on the interaction between an external electric field and the permanent dipoles within the material under investigation. Therefore it is a powerful tool in studying the reorientation dynamics of liquids of small polar molecules. Through measurements of the complex permittivity ($\varepsilon^* = \varepsilon' - i\,\varepsilon''$), it is possible to analyse the dynamics of the dipolar species. In the case of biological solutions, both the solvent (water molecules) and the solute (lysine molecules) contribute to the dielectric signal. As we will see in the following, processes 1 to 3 are related to the reorientation of water dipoles, whereas process 4 is related to the reorientation of lysine dipole molecule. In addition, biological solutions are heterogeneous materials which can cause interfacial polarizations (Maxwell-Vagner type) and it also has free ions or impurities which cause a strong ionic conductivity at high temperatures. We will see that process 5 is a combination of these factors and it also probably contains some dipolar reorientations. In the following we present the experimental results on the lysine-water mixtures, from high to low water contents.

The spectra in figure 1 (and figure S2 in S.I.) look quite complex since several relaxation processes are observed at the different temperatures. Below $T_g$, three dynamical processes are resolved (called processes 1, 2 and 3). As typical in biosystems[30], a high ionic conductivity and/or strong electrode polarization dominates the loss spectra component $\varepsilon''$. This prevents a clear observation of process 3 in $\varepsilon''$, even though it is well-defined in $\varepsilon'$ measurements due to the fact that conductivity does not contribute to this component. To resolve process 3 below $T_g$, we also performed isochronal (figure 2(a)) and TSDC measurements (figure 2(b)), because both these techniques are characterized by a high sensitivity, which allows the detection of weak relaxations observed in isothermal scans[31]. Both measurements reveal the presence of two relaxation processes at temperatures lower than $T_g$, in well-correspondence with processes 2 and 3 observed in the isothermal scans. In addition, at temperatures above $T_g$ the dielectric relaxation measurements (see figure 1(b)) show three dynamical processes (called processes 3, 4 and 5). The dielectric response has the same characteristics for samples with 30 ≤ $c_w$ ≤ 40 wt%. It is important to mention that process 5 has a huge dielectric intensity ($\varepsilon' \sim 10^6$), probably because it is mainly caused by a strong electrode polarization, which is usually displayed in aqueous solutions and wet powders of proteins[30, 32, 33], and an overlapping high ionic conductivity. It is difficult to believe that this large value of the dielectric strength can be caused by a change in a dipole moment due to a molecular reorientation. In spite of the fact lysine at pH = 10 has a net charge of -0.5, which also contributes to an enhancement of the electric dipole moment, there is no dipolar specie in our sample which can cause such a huge intensity of a relaxation process. On the other hand, we have to mention that the freezing in of this process 5 occurs at $T_g$ and it is therefore likely that it also contains a glass transition related relaxation contribution. However, we cannot classify this process as a normal relaxation caused by dipolar species.

Additionally, figure S3 in supplementary information shows the dielectric response at room temperature for different water concentrations. Although in this work we are only focusing on well concentrated solutions (to prevent water crystallization) it should be noted that we obtain a good agreement with the behaviour in the well-diluted regime previously analysed[16]. Focusing on the dielectric parameters corresponding to water relaxation we can estimate an effective hydration number, *Zib*, previously estimated for samples in the well-diluted range. *Zib* is a dynamical hydration number, which reflects the number of water molecules effectively locked by the solute observed by dielectric spectroscopy[34, 35]. For the high concentration range of this study, *Zib* is around 1 or even lower indicating that water

molecules do not show a strong interaction with the solute molecules. This value is much lower than that calculated by Carnevale and Raugei[36] using classical molecular dynamics to form a single hydration layer shell around lysine (12-15 water molecules). However, this simulation explored a concentration range of roughly 0.35 M, whereas in this work we analyse solutions in a high concentration range (see Table I).

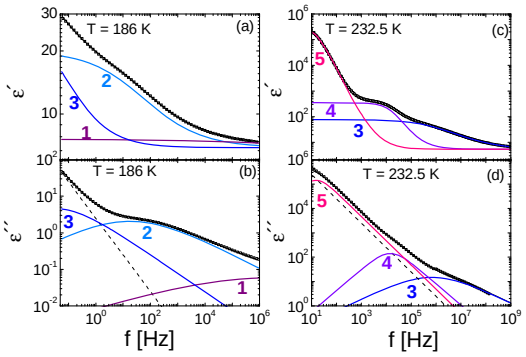


***Figure 1.*** Real ***(a)*** and Imaginary ***(b)*** part of the complex dielectric permittivity ($\varepsilon^*(\omega) = \varepsilon'(\omega) - i\,\varepsilon''(\omega)$) of lysine water solutions ($c_w$ = 40 wt%) at T = 186 K. Solid lines through the data points represent the fits to the experimental data. ***(c) and (d)*** Same as in (a) and (b) but at a temperature higher than $T_g$ (T = 232.5 K). Dashed line in (b) and (d) represents a power law for conductivity.

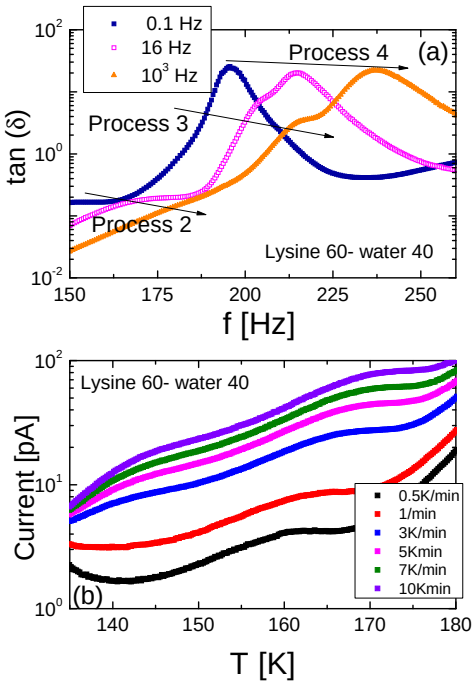


***Figure 2.*** (a) Isochronal dielectric measurements for lysine-water solutions ($c_w$ = 40 wt%). (b) TSDC depolarization current curves for lysine-water solutions ($c_w$ = 40 wt%) at different heating rates.

Now we focus on the water concentration range corresponding to a gel-like sample ($10 \leq c_w < 20$ wt%). For these water levels it is difficult to obtain fully homogeneous samples with a uniform distribution of the water. At $T < T_g$, we can observe the same processes as in the solutions (processes 1, 2 and 3). At higher temperatures ($T > T_g$), the ionic conductivity and/or electrode polarization dominates the response, and due to this limitation we only report the results a few degrees above $T_g$. Finally, we study the lowest water concentration ($c_w$ = 5 wt%) where the sample is a hydrated powder. In this case, a single process at low temperatures is observed, in well correspondence with process 2 observed in the samples of higher water contents. Supplementary Information shows the fittings performed for the samples with $c_w$ = 5 wt% (figure S5).

In conclusion, the dielectric response of both solutions and gel-like samples has 5 different relaxations (processes 1 to 5). In the case of the hydrated powder, a single peak (process 2) is only observed. All the relaxation processes were described by the Cole-Cole equation[29]. Figures S4 and S5 of Supplementary Information show the fittings performed at different temperatures for the samples with $c_w$ = 40 wt% and $c_w$ = 5 wt%. From the fitting, temperature dependences of relaxation times ($\tau$), relaxation strengths ($\Delta\varepsilon$) and shape factors ($\alpha$) were extracted.

**Relaxation times and dielectric strength**

The temperature dependence of the relaxation strength in a dielectric experiment can be used to determine the physical nature of a relaxation process. For a cooperative relaxation (or $\alpha$-relaxation) $\Delta\varepsilon$ decreases with increasing temperature, whereas for a local process (or $\beta$-relaxation) $\Delta\varepsilon$ increases with increasing temperature. In our experiment (see figure 3) $\Delta\varepsilon$ of process 3, (above $T_g$) and processes 4 and 5 decreases with increasing temperature, supporting that all three processes are cooperative in character.

Below $T_g$, there is a strong change in the relaxation strength of process 3 to a value similar to that of process 2. This sudden decrease of its relaxation strength at $T_g$ is also a strong indication of that the physical nature of the relaxation changes at this temperature. However, due to the limited temperature range where this process is visible below $T_g$ we cannot establish a clear temperature dependence of its relaxation strength. This is more easily done for processes 1 and 2, for which it can be established that their relaxation strengths increase with increasing temperature, as expected for local non-cooperative processes. Furthermore, it is clear that the processes 1 and 2, as well as process 3, increase their dielectric strengths with increasing $c_w$, whereas the strengths of processes 4 and 5 decrease with increasing water content (see figures S6 and S3 in supplementary information). This is a powerful indication of that the processes 1, 2 and 3 are caused by dipole reorientations of water molecules, whereas processes 4 and 5 are related to reorientational motions of lysine molecules.

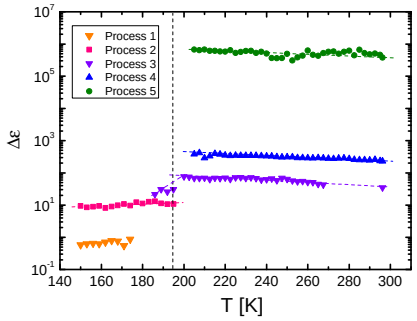


***Figure 3.*** Temperature dependences of the dielectric strengths of processes 1 to 5 of a lysine-water solution ($c_w$ = 40 wt%).

In figure 4(a) the temperature dependences of the relaxation times $\tau$ are shown for $c_w$ = 40 wt% (solution) in filled points together with the relaxation times obtained from TSDC experiments (open points). In addition, data for $c_w$ = 5wt% (hydrated powder) are also included (blue crosses). Finally, figures 4(b) and (c) show the concentration dependence of the relaxation times of processes 2 and 3, respectively. As the main objective of this work is to discuss the water dynamic in the lysine-water system, we are not further discussing processes 4 and 5 related to the motions of the solute molecules.

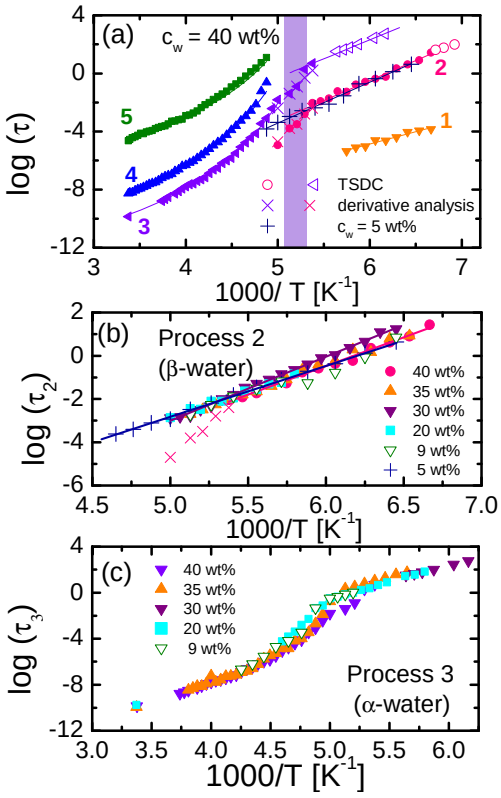


***Figure 4. (a)*** Temperature dependences of the relaxation times of a lysine-water solution ($c_w$ = 40 wt%). Data obtained from isothermal measurements are shown in full points; open points were obtained from TSDC experiments and crosses from the derivative analysis. For comparison we also show relaxation times of the single process 2, observed for the hydrated powder of lysine ($c_w$ = 5 wt%). ***(b)*** Temperature dependences of the relaxation times of process 2 for different hydration levels. ***(c)*** Temperature dependences of the relaxation times of process 3 for different hydration levels.

## DISCUSSION

**Water Dynamics at low temperatures (Lysine-water mixtures)**

Let us first discuss process 1. We observe the characteristic Arrhenius temperature dependence for all the solutions, but it is slightly faster in the case of the gel-like samples. Its intensity increases with increasing water concentration and a minimum quantity of water is necessary to observe it, since it is absent in the hydrated powder ($c_w$ = 5 wt%). This process is commonly observed in different types of water containing systems, including hydrated proteins[37] and water confined in hydrophilic matrices[38], but the origin of this process is not fully clear. In a previous publication[38] we made an attempt to relate this process to the reorientation of hydroxyl groups, since its low activation energy (0.22 eV)[39] is very close to the energy required to break a single hydrogen bond. However, in the present case the activation energy is higher (0.33 eV) and we can only speculate about the origin of this process.

Now we focus on process 2. Below $T_g$, $\tau_2$ exhibits an Arrhenius temperature dependence with an activation energy of 0.48 - 0.53 eV depending on the water concentration[40] (see Table II). From isothermal measurements we cannot assure that process 2 undergoes a dynamic crossover at $T_g$, because the high intensities of the other relaxations, processes 3 and 4, prevent its clear observation in that temperature range. However, by using the derivative analysis[41] of the $\varepsilon'$ component (see figure S7 in Supplementary information) it is clear that process 2 persists and undergoes a dynamical change around $T_g$, when the processes 3 and 4 both enter the experimental window. Moreover, the dielectric strength of process 2 increases with increasing temperature. All these experimental findings are frequently found in so-called secondary- or $\beta$-relaxations of normal glass-forming materials[42]. Hence, this strongly suggests that this relaxation can be identified as a $\beta$-relaxation of water molecules. This is also the only process we can observe in the hydrated powder at $c_w$ = 5 wt%. Another important characteristic is that $\tau_2$ is independent of the water concentration (see figure 4(b)), although a deviation from the Arrhenius behaviour is observed at temperatures close to $T_g$ (crosses in figure 4(a)). This behaviour is commonly seen also for secondary relaxations of pure liquids or polymers when approaching $T_g$.

Let us now move over to process 3. From figures 4(a) and 4(c) it is evident that this process exhibits a dynamic crossover at about the calorimetric $T_g$ from a high temperature Vogel–Fulcher–Tammann (VFT) dependence to an Arrhenius temperature dependence below $T_g$. All the parameters in the VFT equation as well as the activation energy ($E_3$) and log ($\tau_o$) are shown in Table II. $E_3$ is similar to that of process 2, although $\tau_3$ becomes slightly faster with increasing water content, in contrast to $\tau_2$. This suggests that below $T_g$, processes 2 and 3 arise from the same relaxation mechanism.

We now focus on the dynamical crossover of process 3. This type of dynamical crossover at $T_g$ has been observed in several water mixtures with polymers, glass forming liquids, proteins, DNA and peptides by using different experimental techniques[32, 37, 40, 43-

[47]. It has been reported that this crossover is independent of any polypeptide structure, so it is not surprising to find it also in a solution of a single amino acid, as the studied here. In a previous study of short Alanine peptides[48] (di-alanine and tri-alanine), the dynamical transition was not observed. This behaviour was attributed to the lack of structural dependence compared with longer peptides. However, in this study we can confirm the existence of such a crossover even for a single monomer. The reason for the different results is likely that a large part of the water crystallized in Ref. 48, in contrast to the fully amorphous lysine-water solutions studied here. On the other hand, different interpretations of this crossover can be found in the literature and, in fact, its physical origin is still not fully clear. However, most previous studies[33, 37, 40, 43, 44, 49] have indicated that the nature of the water dynamics changes from a cooperative $\alpha$-like relaxation to a more local $\beta$-like relaxation below the crossover temperature. Thus, the more cooperative and viscosity related motions in the hydration water seem to vanish at $T_g$. Moreover, as far as we are aware of it has never been observed for any hydrated material that $\alpha$-water (i.e. process 3) continues after the crossover to $\beta$-water (i.e. process 2) has occurred, and that this $\alpha$-water at a lower temperature and slower time scale shows a crossover to a slower $\beta$-like process. Thus, processes 2 and 3 have never been simultaneously observed at any temperature. As the crossover of $\alpha$-water is produced at $T_g$ it seems likely that it is due to confinement effects caused by the freezing in of the molecular movements of lysine[22, 40]. Hence, the more long-range and cooperative water motions may disappear due to the confinement the "freezing-in" of the lysine relaxations causes.

Following the above discussion, we can conclude that in lysine-water solutions three different relaxations (processes 1 to 3) results from the motion of water molecules. This is not a common behaviour, neither in hydrated protein powders[22, 33, 50] nor in small peptides[14], where only two processes are observed below $T_g$. It should be mentioned that in a study of hydrated powders of bovine serum albumin, Shinyasiki et al[32] observed four processes below $T_g$ but only two of them are originated from hydration water (the other two are due to crystallized bulk water). Thus, the greatest advantage of the L-lysine-water system studied here is the possibility to cover a large concentration range ($c_w$ varying between 5 and 40 wt%) from a hydrated powder to a clear and transparent solution, without any crystallization on cooling/heating. This contrasts the possibility of protein or peptide studies, where only hydrated powders can be explored at low temperatures without crystallization. Therefore in the present system we can clearly recognize the characteristics of each relaxation process. Below $T_g$, process 2 is identified as a $\beta$-relaxation of water molecules, whereas process 3 displays the same temperature dependence as process 2, suggesting a similar origin of the two relaxation mechanisms. Above $T_g$, process 3 is identified as a cooperative $\alpha$-relaxation of water molecules. It is here worth to mention that living cells contain about 70 wt% of water, and therefore these results have strong impact on the characterization of water dynamics in biological environments. Our results suggest that water splits into three different dielectric relaxations at low temperatures and this multi-fold dynamics distinguish biological solutions somewhat from other kinds of solutions, where only two water processes can be observed.

***Table II.*** Activation energy and pre-exponential factor obtained from the Arrhenius dependences of processes 2 and 3 below Tg. $E_a$ is the activation energy and $\log(\tau_o)$ is the pre-exponential factor. Average errors are 0.02 and 0.03 for $E_a$ and $\log(\tau_o)$ respectively. VFT parameters for process 3 are given above $T_g$.

| Sample | Process 2 (β-water) | | Process 3 (α-water) below $T_g$ | | | Process 3 (α-water) above $T_g$ | |
|---|---|---|---|---|---|---|---|
| | Ea [eV] | $\log(\tau_o)$ | Ea [eV] | $\log(\tau_o)$ | D | $\log(\tau_o)$ | To (K) |
| L60-W40 | 0.52 | -16.37 | 0.51 | -12.97 | 7.86 | -13.39 | 154.08 |
| L65-W35 | 0.53 | -16.27 | 0.55 | -13.99 | 5.33 | -12.50 | 167.62 |
| L70-W30 | 0.53 | -17.90 | 0.54 | -14.01 | 4.50 | -11.77 | 171.10 |
| L80-W20 | 0.48 | -14.82 | 0.57 | -14.96 | --- | --- | --- |
| L91-W09 | 0.48 | -14.87 | --- | --- | --- | --- | --- |
| L95-W05 | 0.48 | -14.91 | --- | --- | --- | --- | --- |

**Comparison with hard-confinement systems**

For water in hard confinements a nearly universal water relaxation is commonly observed, and the characteristics and time scale of it is basically identical to process 2 in the present study. The relaxation times of the main water relaxation previously observed in two well defined confinement systems, graphite oxide (GO)[51] and MCM-41[9], do not show any significant concentration dependence (see figure 5(a)). This behaviour resembles the concentration dependences we here observe for processes 2 and 3 (below $T_g$) (see figures 4 (b) and (c)). However, below we will show that it contrasts the behaviour of water confined in ordinary solutions.

For water in hard confinements a dynamic crossover is observed at a certain temperature and time-scale. According to our interpretation this dynamic crossover can be explained by finite size effects. Following the Adam-Gibbs theory[52], the size of a cooperative region increases with decreasing temperature. When the cooperative region reaches a certain size (determined by the size of the confinement) the dynamics change to a thermally activated Arrhenius temperature dependent $\beta$-like relaxation process. Since the calorimetric glass transition temperature corresponds to the temperature for which the structural ($\alpha$) relaxation time reaches a time-scale of the order of 100 s, and this time-scale is never reached due to the confinement induced dynamical crossover, $T_g$ cannot be experimentally detected by DSC[6, 18, 47, 51-54]. Thus, the $\alpha$-relaxation vanishes before it reaches the time-scale of a glass transition, and this has been experimentally verified by several previous studies. Since the relaxation time of this water process does not show a strong dependence on the water content below the crossover temperature it can be considered as an intrinsic $\beta$-relaxation of the confined water. Thus, despite that the present solutions are very different compared to water in hard confinements it is evident that the characteristics of process 2 is almost identical to this "universal" $\beta$-relaxation of supercooled water in hard confinements. Also the behaviour of process 3 is similar below $T_g$, although its relaxation time is slower and its dynamic crossover is caused by the glass transition of the solution, as in the case of ordinary solutions, discussed below. The similar activation energies of processes 2 and 3 suggest, however, that they have the same physical nature.

### Comparison with ordinary solutions

Ordinary solutions are commonly showing two dielectric processes; the glass transition related structural $\alpha$-relaxation (above $T_g$) and a relaxation due to water molecules (which can be observed both below and above $T_g$) [16, 18, 19, 34, 50-53]. At $T_g$ the relaxation time of water changes from a high temperature non-Arrhenius behaviour to an Arrhenius dependence below $T_g$. This change in the dynamics is more favourably observed at high water concentrations, when water molecules to a large extent are surrounded by other water molecules. The concentration dependence of the water relaxation time in ordinary solutions is much stronger than that observed in hard confinements (see figure 5(b)). This concentration dependence is probably obtained because water in ordinary solutions is sensitive to the specific details of the water-solute interactions. Furthermore, at low water concentrations the $\beta$-relaxation of the solute molecules may contribute to this water relaxation[18,53]. However, at high water concentrations of most solutions the relaxation times collapse onto the same single curve[40] (with an activation energy of about 0.54 eV) as observed for water in hard confinements.

The dynamics of water in hard confinements was easily compared with process 2 in the lysine solutions. Now, we want to make a comparison between the results observed here and the results of ordinary solutions. What is clear is that in ordinary solutions there are only up to two relaxations due to motions of water molecules (always process 3 and for larger solute molecules generally also process 1) and this contrasts the presence of three water relaxations in lysine solutions. Process 3 ($\alpha$-water) in lysine solutions exhibits a dynamic crossover at $T_g$ and it is considerably slower than the intrinsic $\beta$-relaxation of water (process 2). This process 3 is comparable with the main water relaxation in ordinary solutions. The only significant difference is that above $T_g$ the here observed $\alpha$-water (process 3) does not seem to include any contribution from the solute molecules, in contrast to most aqueous solutions. On the other hand, process 2 in lysine solutions, i.e. the intrinsic $\beta$-relaxation of water, seems to be absent in ordinary solutions. The reason for this is not fully clear, but if the intrinsic $\beta$-relaxation of water is of Johari-Goldstein type[54] it should require that a few water molecules are hydrogen bonded to each other, and this implies that it would not occur at very low water concentrations where such "water clusters" are unlikely to be formed. Since it is normally only at such low water concentrations the observed $\beta$-like water relaxation is considerably slower than the intrinsic $\beta$-relaxation of water, the two similar water relaxations cannot be separated at high water concentrations. In fact, as mentioned above, the $\beta$-like water relaxation in ordinary solutions of high water concentrations cannot even be distinguished from the intrinsic $\beta$-relaxation of water.

### Three water processes

Finally, we emphasize that supercooled water in lysine solutions show three dielectric relaxations at temperatures below $T_g$ (processes 1, 2 and 3). This has not been observed for supercooled water in other systems previously investigated. The reason for this is probably that sufficiently large units of water are present to give rise to the intrinsic $\beta$-relaxation of water already at low water contents, i.e. the water molecules may not be uniformly distributed at low water contents. At higher water contents this intrinsic $\beta$-relaxation is complemented with process 3, which below $T_g$ should be caused by the $\beta$-like relaxation of the remaining water, i.e. the water that is too much influenced by the solute molecules, both structurally and dynamically, to participate in the intrinsic $\beta$-relaxation of water. This interpretation would also explain why process 3 shows a weaker concentration dependence than the main water relaxation in ordinary aqueous solutions, since in the latter case process 3 will basically "transform" to process 2 with increasing water content, whereas in the present system process 3 will only involve the water molecules strongly influenced by the lysine molecules.

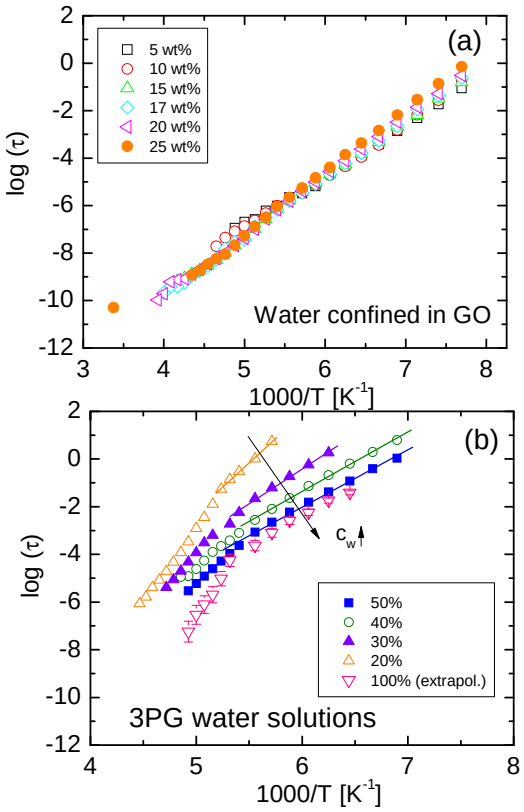


***Figure 5.*** (a) Concentration dependence of the temperature dependence of the relaxation time of water in a hard confinement (graphite oxide from reference[51]). (b) Same as in (a) for water in a soft confinement (tri-propylene glycol-water solutions)[55]. In both cases, a crossover from non-Arrhenius to Arrhenius at $T_g$ (for solutions) and at a certain temperature (for hard confinement) is observed.

## Conclusions

In this dielectric relaxation study of supercooled lysine-water solutions we observed five different relaxation processes; three of them were due to motions of water molecules, and present below $T_g$. From the results we can state that these biological solutions show some important differences compared to "ordinary" aqueous solutions. In these biological solutions a decoupling of

$\beta$-like and $\alpha$-like relaxations is observed slightly above $T_g$, and this has not been seen for ordinary solutions. Hence, this behaviour may distinguish biological solutions from other kinds of solutions.

In addition, in the case of hydrated proteins it has to our knowledge never been observed that the $\alpha$-like relaxation process of the hydration water continues into the low temperature range where the Arrhenius temperature dependent $\beta$-relaxation of water can be observed. Thus, hydration water of proteins, and, in fact, also water in solid confinements, exhibit a dynamic crossover around 180 K from a $\alpha$-like relaxation above the crossover temperatures to the "universal" $\beta$-relaxation at lower temperatures, with no indication of a continuation of the $\alpha$-like relaxation to temperatures below the crossover temperature. Hence, in the case of the lysine-water solutions we have a decoupling of the "universal" $\beta$-relaxation of water from its $\alpha$-like relaxation, rather than a dynamic crossover. However, also this $\alpha$-like relaxation of the water transforms to a $\beta$-like process at the calorimetric and dielectric glass transition temperature of lysine.

## Acknowledge

S.C. acknowledges funding by the Basque Government (SAIOTEK S-PE13IV001 and project IT-654-13), and the Spanish Ministry of Education (project MAT2012-31088). J.S. thanks the Swedish Research Council and the Swedish Energy Agency for financial support.

## Notes and references

[a] *Centro de Física de Materiales- Material Physics Centre (MPC), CSIC-Universidad del País Vasco (UPV/EHU, Paseo Manuel de Lardizabal 5 (20018), San Sebastian, Spain; E-mail:scerveny@ehu.es*
[b] *Donostia International Physics Center, Paseo Manuel de Lardizabal 4, San Sebastián, Spain*
[c] *Department of Applied Physics, Chalmers University of Technology, SE-412 96 Göteborg, Sweden. E-mail:jan.swenson@chalmers.se*

† Electronic Supplementary Information (ESI) available: [Calorimetric response of samples with high water content, dielectric spectra in the GHz region, details of fitting procedures for sample with $c_w$ = 40 wt% and $c_w$ = 5 wt% and derivative analysis of the sample with $c_w$ = 40 wt% are available]c. See DOI: 10.1039/b000000x/

1. M. Chaplin, *Nat. Rev. Mol. Cell Biol.*, 2006, **7**, 861-866.
2. H. Frauenfelder, P. W. Fenimore, G. Chen and B. H. McMahon, *Proceedings of the National Academy of Sciences of the United States of America*, 2006, **103**, 15469-15472.
3. P. Ball, *ChemPhysChem*, 2008, **9**, 2677-2685.
4. M. E. Johnson, C. Malardier-Jugroot, R. K. Murarka and T. Head-Gordon, *Journal of Physical Chemistry B*, 2009, **113**, 4082-4092.
5. H. Frauenfelder, G. Chen, J. Berendzen, P. W. Fenimore, H. Jansson, B. H. McMahon, I. R. Stroe, J. Swenson and R. D. Young, *Proceedings of the National Academy of Sciences of the United States of America*, 2009, **106**, 5129-5134.
6. D. Nerukh and S. Karabasov, *The Journal of Physical Chemistry Letters*, 2013, **4**, 815-819.
7. S. Takahara, M. Nakano, S. Kittaka, Y. Kuroda, T. Mori, H. Hamano and T. Yamaguchi, *Journal of Physical Chemistry B*, 1999, **103**, 5814-5819.
8. A. Faraone, L. Liu, C. Y. Mou, C. W. Yen and S. H. Chen, *Journal of Chemical Physics*, 2004, **121**, 10843-10846.
9. J. Sjostrom, J. Swenson, R. Bergman and S. Kittaka, *Journal of Chemical Physics*, 2008, **128**, 154503.
10. S. Cerveny, G. A. Schwartz, J. Otegui, J. Colmenero, J. Loichen and S. Westermann, *Journal of Physical Chemistry C*, 2012, **116**, 24340-24349.
11. A. K. Soper, *Journal of Physics-Condensed Matter*, 2012, **24**.
12. C. Malardier-Jugroot, M. E. Johnson, R. K. Murarka and T. Head-Gordon, *Physical Chemistry Chemical Physics*, 2008, **10**, 4903-4908.
13. D. Russo, J. Teixeira and J. Ollivier, *Journal of Chemical Physics*, 2009, **130**, 235101.
14. S. E. Pagnotta, S. Cerveny, A. Alegria and J. Colmenero, *Physical Chemistry Chemical Physics*, 2010, **12**, 10512-10517.
15. S. Perticaroli, L. Comez, M. Paolantoni, P. Sassi, A. Morresi and D. Fioretto, *Journal of the American Chemical Society*, 2011, **133**, 12063-12068.
16. I. Rodriguez-Arteche, S. Cerveny, A. Alegria and J. Colmenero, *Physical Chemistry Chemical Physics*, 2012, **14**, 11352-11362.
17. S. Cerveny, J. Colmenero and A. Alegria, *European Physical Journal-Special Topics*, 2007, **141**, 49-52.
18. a. M.-L. L. S Diaham, *J. Phys. D: Appl. Phys.*, 2013, **46** 185302
19. K. Elamin, J. Sjostrom, H. Jansson and J. Swenson, *Journal of Chemical Physics*, 2012, **136**, 104508.
20. N. Shinyashiki, M. Shinohara, Y. Iwata, T. Goto, M. Oyama, S. Suzuki, W. Yamamoto, S. Yagihara, T. Inoue, S. Oyaizu, S. Yamamoto, K. L. Ngai and S. Capaccioli, *Journal of Physical Chemistry B*, 2008, **112**, 15470-15477.
21. L. Comez, L. Lupi, A. Morresi, M. Paolantoni, P. Sassi and D. Fioretto, *Journal of Physical Chemistry Letters*, 2013, **4**, 1188-1192.
22. H. Jansson and J. Swenson, *BBA-Proteins Proteomics*, 2010, **1804**, 20-26.
23. S. Sinha, D. H. J. Lopes and G. Bitan, *ACS Chemical Neuroscience*, 2012, **3**, 473-481.
24. S. W. Sauer, S. Opp, G. F. Hoffmann, D. M. Koeller, J. G. Okun and S. Kolker, *Brain*, 2011, **134**, 157–170.
25. V. G. Bhoj and Z. J. Chen, *Nature*, 2009, **458**, 430-437.
26. L. Hong, N. Smolin, B. Lindner, A. P. Sokolov and J. C. Smith, *Physical Review Letters*, 2011, **107**.
27. W. Doster, *BBA-Proteins Proteomics*, 2010, **1804**, 3-14.
28. S. Khodadadi, A. Malkovskiy, A. Kisliuk and A. P. Sokolov, *BBA-Proteins Proteomics*, 2010, **1804**, 15-19.
29. K. S. Cole and R. H. Cole, *Journal of Chemical Physics*, 1942, **10**, 98-105.
30. M. Wolf, R. Gulich, P. Lunkenheimer and A. Loidl, *Biochim. Biophys. Acta-Gen. Subj.*, 2011, **1810**, 727-740.
31. V. Samouillan, D. Tintar and C. Lacabanne, *Chemical Physics*, 2011, **385**, 19-26.
32. N. Shinyashiki, W. Yamamoto, A. Yokoyama, T. Yoshinari, S. Yagihara, R. Kita, K. L. Ngai and S. Capaccioli, *The Journal of Physical Chemistry B*, 2009, **113**, 14448-14456.
33. J. Swenson, H. Jansson and R. Bergman, *Physical Review Letters*, 2006, **96**, 247802.
34. G. T. H. Richard Buchner, and Peter M. May, *J. Phys. Chem. A*, 1999, **103**, 1-9.
35. T. Sato, R. Buchner, S. Fernandez, A. Chiba and W. Kunz, *J. Mol. Liq.*, 2005, **117**, 93-98.
36. V. Carnevale and S. Raugei, *The Journal of Chemical Physics*, 2009, **131**, -.
37. H. Jansson, R. Bergman and J. Swenson, *Journal of Physical Chemistry B*, 2011, **115**, 4099-4109.
38. M. Monasterio, H. Jansson, J. J. Gaitero, J. S. Dolado and S. Cerveny, *The Journal of Chemical Physics*, 2013, **139**, 164714.
39. L. Pauling, *The Natural of the Chemical Bond and the Structure of Molecules and Crystal*, Cornell University Press, New York, 1960.
40. S. Cerveny, A. Alegria and J. Colmenero, *Physical Review E*, 2008, **77**, 031803.

41. M. Wübbenhorst and J. van Turnhout, *Journal of Non-Crystalline Solids*, 2002, **305**, 40-49.
42. K. L. Ngai, *Relaxation and Diffusion in Complex Systems (Partially Ordered Systems)*, Springer, 2011.
43. M. Vogel, *Physical Review Letters*, 2008, **101**, 225701.
44. A. Panagopoulou, A. Kyritsis, N. Shinyashiki and P. Pissis, *Journal of Physical Chemistry B*, 2012, **116**, 4593-4602.
45. S. Magazu, F. Migliardo and A. Benedetto, *Journal of Physical Chemistry B*, 2010, **115**, 7736-7743.
46. W. Doster, S. Busch, A. M. Gaspar, M. S. Appavou, J. Wuttke and H. Scheer, *Physical Review Letters*, 2010, **104**, 098101
47. C. R. Herbers, D. Sauer and M. Vogel, *Journal of Chemical Physics*, 2012, **136**.
48. Y. F. He, P. I. Ku, J. R. Knab, J. Y. Chen and A. G. Markelz, *Physical Review Letters*, 2008, **101**.
49. M. Vogel, *Journal of Physical Chemistry B*, 2009, **113**, 9386-9392.
50. S. A. Lusceac, M. Rosenstihl, M. Vogel, C. Gainaru, A. Fillmer and R. Bohmer, *Journal of Non-Crystalline Solids*, 2011, **357**, 655-663.
51. S. Cerveny, F. Barroso-Bujans, A. Alegria and J. Colmenero, *Journal of Physical Chemistry C*, 2010, **114**, 2604-2612.
52. G. Adam and J. H. Gibbs, *Journal of Chemical Physics*, 1965, **43**, 139.
53. B. S. A. D. Sauer, M. Rosenstihl, S. Schneider, V. Talluto, T. Walther, T. Blochowicz, B. Stühn, M. Vogel, *J. Chem. Phys.*, 2014, **140**, 114503
54. G. P. Johari and M. Goldstein, *Journal of Chemical Physics*, 1970, **53**, 2372-&.
55. S. Cerveny, G. A. Schwartz, A. Alegria, R. Bergman and J. Swenson, *Journal of Chemical Physics*, 2006, **124**, 194501.